Quantitative proteomic analysis reveals that Luks-PV exerts antitumor activity by regulating the key proteins and metabolic pathways in HepG2 cells

Chang-Cheng Zhao, Wen-Wei Yu, Ying-Jie Qi, Liang-Fei Xu, Zi-Ran Wang, Ya-Wen Qiang, Fan Ma and Xiao-Ling Ma

Hepatocellular carcinoma (HCC) is a complicated and poor prognosis cancer, necessitating the development of a potential treatment strategy. In this study, we initially revealed that LukS-PV belonged to leukocidin family performs an anti-HCC action. Then, we used liquid chromatography-mass spectrometry (LC/MS) to compare protein expression profiles of the LukS-PV-treated human HCC cell lines HepG2 and the control cells. GO annotations and Kyoto Encyclopedia of Genes and Genomes pathway analysis were carried out of differential expression followed by protein–protein interactome, to explore the underlying cancer suppressor mechanisms of LukS-PV for human HCC. A total of 88 upregulated proteins and 46 downregulated proteins were identified. The top 10 proteins identified by the MCC method are FN1, APP, TIMP1, nucleobindin-1, GOLM1, APLP2, CYR61, CD63, ENG, and CD9. Our observation on protein expression indicated that LukS-PV produces a signature affecting central carbon metabolism in cancer, galactose metabolism, and fructose and mannose metabolism pathways. The results give a functional effects and molecular mechanism insight, following LukS-PV treatment. ***Anti-Cancer Drugs*** **31:223–230 Copyright © 2019 The Author(s). Published by Wolters Kluwer Health, Inc.**

Anti-Cancer Drugs 2020, **31:**223–230

Keywords: hepatocellular carcinoma, Luks-PV, quantitative proteomics, tandem mass tag

Division of Life Sciences and Medicine, The First Affiliated Hospital of USTC, University of Science and Technology of China, Hefei, Anhui, China

Correspondence to Xiao-Ling Ma, PhD, Division of Life Sciences and Medicine, The First Affiliated Hospital of USTC, University of Science and Technology of China, Hefei, Anhui 23000, China
Tel: +86 18949895015; fax: +86 551 6336 2933;
e-mail: maxiaoling@ustc.edu.cn

Received 20 July 2019 **Revised form accepted** 25 October 2019

Introduction

Hepatocellular carcinoma (HCC) is the most common form of liver cancer. As the second leading cause of global cancer mortality, HCC endangers over 780 000 new patients per year [1]. Although many treatment methods are available for HCC, including surgical resection, liver translation, radioembolization, radiation therapy, and molecularly targeted therapies [2], five-year survival rate of HCC patients remains dismal. Therefore, further efforts to develop new treatment strategy of patients with HCC are needed.

LukS-PV is one of the two components of Panton–Valentine leucocidin (PVL), which is a pore-forming leukocidin secreted by *Staphylococcus aureus*. It has increasingly been recognized to have a potential role for treating acute myeloid leukemia (AML). For example, our previous work demonstrated that LukS-PV potently promoted differentiation and induced apoptosis in THP-1 cells [3,4]. Additionally, we found that LukS-PV could induce differentiation of human AML cells, including AML cell lines and primary AML blasts [5,6]. Accordingly, we speculated that LukS-PV plays a role in HCC progression, which has been validated our unpublished observations.

Proteomics is a powerful technology that can help identify therapeutic targets and potential biomarkers in different diseases. In this study, we utilized this high throughput technology to identify differentially expressed proteins (DEPs) in LukS-PV-treated HepG2 cells relative to the untreated control. These data were then analyzed using bioinformatics and multiple pathways and a number of molecular functions were implicated to play a role in anticancer effect. Overall, this research provides a novel understanding of the mechanisms of anticancer in HCC.

Experimental procedures

Cell culture

Human HCC cell lines HepG2 was purchased from the Institute of Biochemistry and Cell Biology, Chinese Academy of Sciences (Shanghai, China) and cultured in RPMI 1640 medium (Gibco, California, USA) supplemented with 10% fetal bovine serum (Gibco), 100 U/ml

Supplemental Digital Content is available for this article. Direct URL citations appear in the printed text and are provided in the HTML and PDF versions of this article on the journal's website, www.anti-cancerdrugs.com.

0959-4973 Copyright © 2019 The Author(s). Published by Wolters Kluwer Health, Inc. DOI: 10.1097/CAD.0000000000000866

penicillin and 100 µg/ml streptomycin (Invitrogen, USA) at 37°C in a humidified incubator air with 5% CO_2.

Recombinant LukS-PV production and purification

pET28a (Roche Diagnostics Corp, Basel, Switzerland) was used to produce recombinant hexa-His-tagged LukS-PV. The sequence was amplified from PVL-positive *S. aureus* isolates. PCR products were digested with XhoI and BamHI (Promega, Madison, Wisconsin, USA) and ligated into the pET28a vector. Recombinant LukS-PV purification was described previously by Sun *et al*. [3].

Cell proliferation, apoptosis, and invasion assays

Cell proliferation assays, apoptosis, and invasion assays were performed as described previously [3,7].

Western blot assay

Western blotting was performed and analyzed as described previously [8]. The following antibodies were used: β-actin (Abcam), E-cadherin, vimentin, SNAIL (Cell Signaling Technology), N-cadherin, MMP-9, and MMP-2 (Proteintech).

Protein digestion and TMT labeling

Samples were subjected to the filter-assisted sample preparation (FASP) protocol [9]. Processed samples were subsequently transferred to a fresh tube and subjected to tryptic digestion overnight at 37°C. The resulting peptides were dried completely in a vacuum concentrator and stored at –80°C. Tandem Mass Tag (TMT) labeling was performed following the manufacturer's protocol in the TMTsixplex Isobaric Label Reagent Set. Briefly, tryptic peptides was reconstituted in 100 µl of 50 mM TEABC buffer and mixed with the TMT reagent reconstituted in 41 µl anhydrous acetonitrile and incubated at 25°C for 1 hour. All labeled peptides were mixed, completely dried in a vacuum concentrator and stored at –80°C.

Quantitative analysis using liquid chromatography-mass spectrometry

The TMT-labeled peptides were resuspended in 0.1% formic acid and analyzed on an AB Sciex TripleTOF 5600 mass spectrometer (AB SCIEX; Concord, ON, Canada) with a NanoAcquity UPLC (Waters, Milford, Massachusetts, USA) system as previously described [10]. The generated data were analyzed using ProteinPilot version 4.5 software. The dataset was searched using the following parameters: cysteine carbamidomethylation and TMT labeling as fixed modifications, methionine oxidation as a variable modification and digestion by trypsin with at least two missed cleavages. The identified proteins with at least two peptide matches and a confidence threshold >99% were further analyzed. Proteins were determined to be differentially expressed if ≥1.50 or ≤0.667 of fold change was noted and if a P value <0.05 was obtained.

Real-time RT-PCR analysis

The proteomic data were validated utilizing SYBR Green-based real-time quantitative PCR (qPCR) performed on Roche Cobas z 480 analyzer. Five hundred nanogram of total RNA from each sample was used to synthesize first-strand cDNA using a PrimeScript II 1st strand cDNA synthesis kit (Takara) in accordance with the manufacturer's recommendations. Primers used in this article are shown in Supplementary Table 1, Supplemental digital content 1, *http://links.lww.com/ACD/A321*. The comparative Ct ($2^{-\Delta\Delta Ct}$) method was used to quantify expression of genes, and fold change was used to present data. β-actin was used as a reference gene.

Bioinformatics analysis

GO annotations and Kyoto Encyclopedia of Genes and Genomes (KEGG) pathway analysis of altered proteins were analyzed with OmicsBean (http://www.omicsbean.cn/) [11].

Protein–protein interactome network construction and module analysis

The Search Tool for the Retrieval of Interacting Genes (STRING) database (http://string.embl.de/) was evaluated the interactive relationships among DEPs. A combined score >0.4 was set as the cutoff criterion. Then, we used Cytoscape Version 3.7.1 to visualize the biomolecular interaction networks of the DEPs. Molecular Complex Detection (MCODE) plugin was used to screen modules from the PPI network with degree cutoff 2, haircut on, node score cutoff 0.2, k-score 2, maximum depth 100, and nodes more than 8. The functional and pathway enrichment analysis was performed through DAVID in the modules.

Results

Apoptosis, proliferation, invasion and metastasis effects of LukS-PV on HepG2 cells

First, we set out to investigate whether LukS-PV influences on the biological behavior changes of HCC. We observed that LukS-PV promoted apoptosis (Fig. 1a) and inhibited proliferation (Fig. 1b) in the treated HepG2 cells *in vitro* as compared with its counterpart. In addition, the capacity of invasiveness effect was significantly impaired concerning LukS-PV (Fig. 1c). Because Epithelial-Mesenchymal Transition (EMT) has long been considered as a crucial step for metastasis initiation [12], several biomarkers of the EMT phenotype were detected using western blotting. We found that LukS-PV suppressed EMT in HCC cells, manifesting as down-regulation of N-cadherin, MMP-2, MMP-9, Snail, and Vimentin expression, and upregulation of E-cadherin expression (Fig. 1d). These findings suggested that LukS-PV exerts antitumor activity in HepG2 cells, and it has therapeutic promise to inhibit HCC progression.

Fig. 1

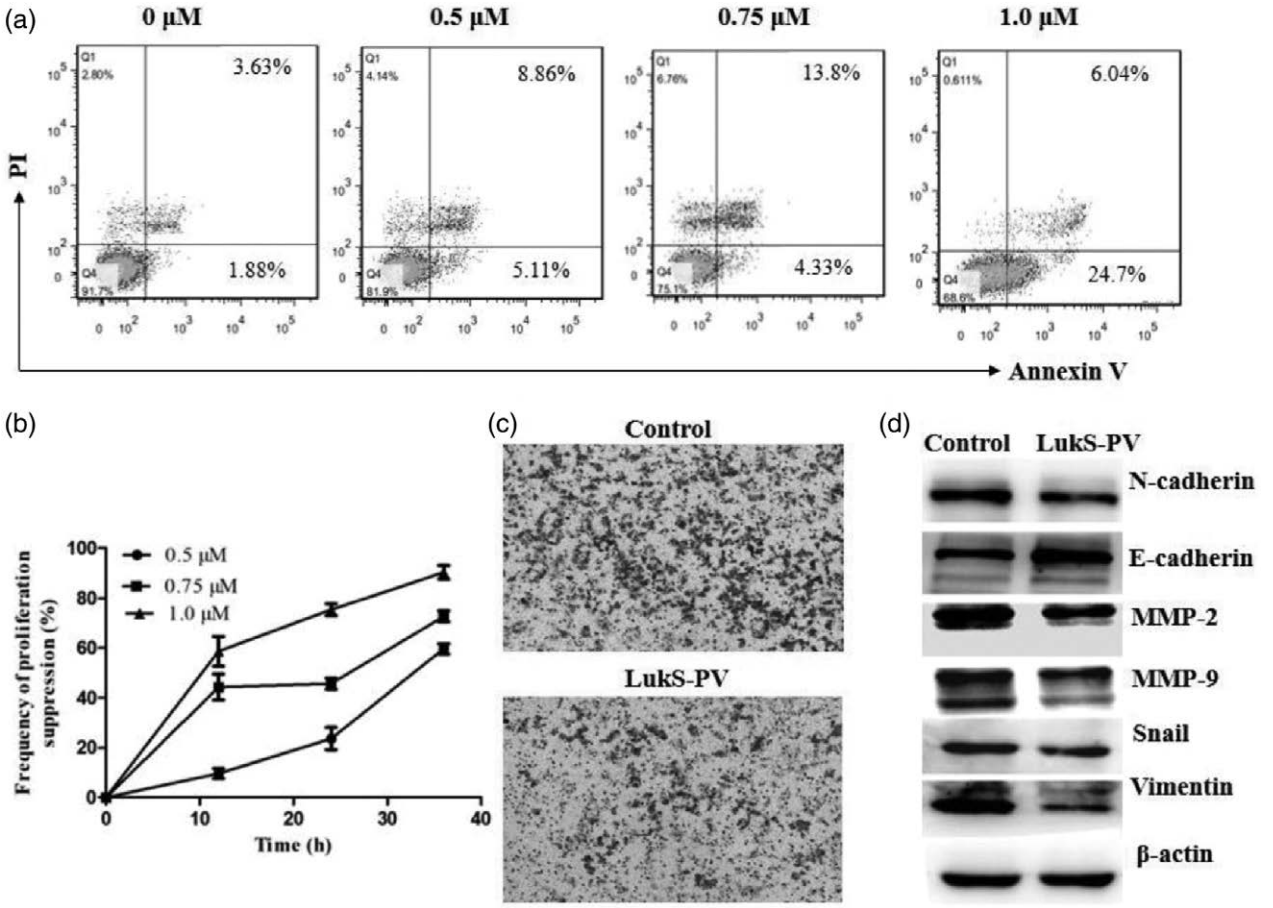

LukS-PV promotes the apoptosis and suppresses tumor proliferation, invasion and metastasis in HepG2 cells. (a) HepG2 cells were exposed to different concentrations (0, 0.5, 0.75, 1.0 μM) of LukS-PV for 24 hours. Apoptosis was quantified by fluorescence-activated cell sorting (FACS) analysis stained with Annexin-FITC and PI-PE. (b) MTT assay was performed to determine the proliferation of HepG2 cells with 0.5, 0.75, 1.0 μM concentration of LukS-PV treatment, respectively. (c) Inhibitory effects of LukS-PV on the invasion of HepG2 cells. HepG2 cells were treated with 1.0 μM LukS-PV for 24 hours, and invasiveness of control cells and cells treated with 1.0 μM LukS-PV was observed using Transwell assay. (d) Western blot analysis of EMT markers in HepG2 cells with LukS-PV (1.0 μM). β-actin was used as an equal loading control.

Table 1 **The top 10 upregulated differentially expressed proteins in LukS-PV-treated HepG2 cells**

Protein accession	Protein description	Luks/Ctr ratio	Luks/Ctr *P* value	Protein name
P13196	5-aminolevulinate synthase, nonspecific, mitochondrial	6.908	0.00020359	ALAS1
Q13772	Nuclear receptor coactivator 4	4.503	0.00064111	NCOA4
Q06481	Amyloid-like protein 2	4.44	1E-32	APLP2
Q9BXS4	Transmembrane protein 59	4.357	0.00061755	TMEM59
P05067	Amyloid-beta A4 protein	4.259	1.62437E-12	APP
Q86VP1	Tax1-binding protein 1	4.043	1.59406E-12	TAX1BP1
Q9Y287	Integral membrane protein 2B	3.965	0.002558	ITM2B
Q96QD8	Sodium-coupled neutral amino acid transporter 2	3.407	0.00042052	SLC38A2
Q9NZV1	Cysteine-rich motor neuron 1 protein	3.302	0.00055943	CRIM1
Q13641	Trophoblast glycoprotein	3.123	1.80342E-05	TPBG

Identification of differentially expressed proteins in LukS-PV-treated HepG2 cells

To understand the cancer suppressor mechanism of LukS-PV, then we performed a comparative study on the protein profiles labeled with TMT between LukS-PV-treated HepG2 cells and the untreatment cells by means of mass spectrometry. For global proteome analysis, 6150 proteins were identified and 5445 proteins were quantified in HepG2 cells. Filtered with threshold value of expression fold change (fold change ≥1.50 or ≤0.667) and *P* value <0.05, among which 134 DEPs were picked up, with 88 proteins upregulated and 46 downregulated. Of the dysregualted proteins, the most upregulated protein was ALAS1, with a fold change of more than 6.9, and the

Table 2 The top 10 downregulated differentially expressed proteins in LukS-PV-treated HepG2 cells

Protein accession	Protein description	Luks/Ctr Ratio	Luks/Ctr *P* value	Protein name
Q15004	PCNA-associated factor	0.305	8.4086E-07	PCLAF
P07305	Histone H1.0	0.361	1.4705E-07	H1F0
Q9BRK5	45 kDa calcium-binding protein	0.457	0.022718	SDF4
Q02818	Nucleobindin-1	0.462	7.1989E-07	NUCB1
P16401	Histone H1.5	0.486	0.000022617	HIST1H1B
Q9BZD4	Kinetochore protein Nuf2 2	0.494	0.0004782	NUF2
P16402	Histone H1.3	0.498	0.0110831	HIST1H1D
Q6PJG6	BRCA1-associated ATM activator 1	0.516	0.00068191	BRAT1
Q9BZL1	Ubiquitin-like protein 5	0.52	0.00170196	UBL5
Q9H173	Nucleotide exchange factor SIL1	0.528	0.00167586	SIL1

Fig. 2

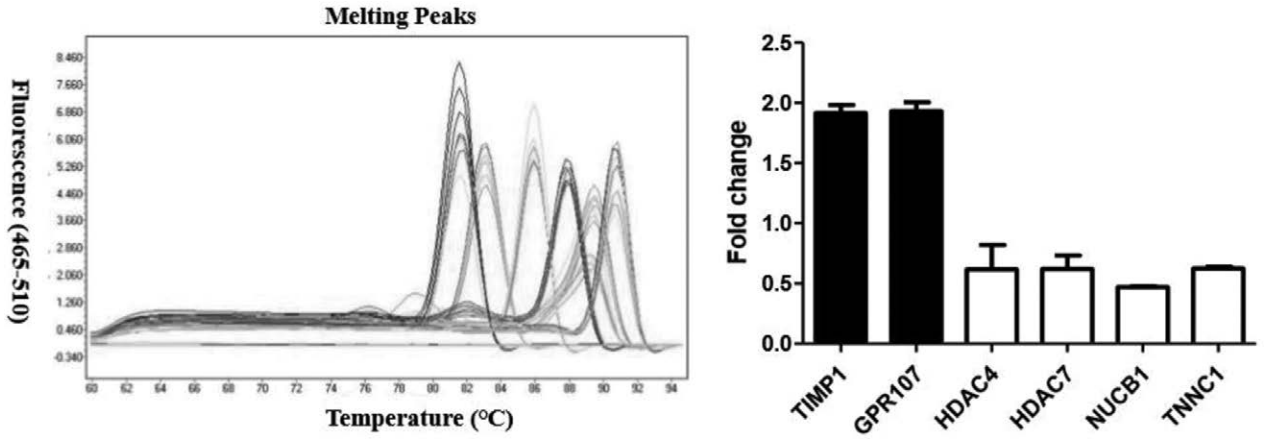

Validation of proteomic results using real-time RT-PCR. Six differentially expressed proteins were validated by qPCR. The expression of six proteins (TIMP1, GPR107, HDAC4, HDAC7, NUCB1, and TNNC1) selected from proteomics result between Luks-PV stimulated and unstimulated HepG2 cell was performed using real-time RT-PCR method.

most downregulated was PCLAF, with a fold change of less than 0.5. The top 10 upregulated and downregulated DEPs were listed in Tables 1 and 2, respectively, providing a wide source of target proteins for further study in LukS-PV regulation. These data are essential to better understand the exact regulation of LukS-PV and also provides ideas for HCC clinical treat.

Validation of proteomic analysis by real-time RT-PCR

To validate the results measured by TMT-based quantitative proteomics analysis, a subset of six genes [TIMP1, GPR107, HDAC4, HDAC7, nucleobindin-1 (NUCB1), and troponin C1 (TNNC1)] was selected and analyzed by real-time RT-PCR combined with our future research interests. The results showed that the metalloproteinase inhibitor 1 (TIMP1), and a G-protein-coupled receptor (GPR107) was upregulated in the Luks-PV-treated HepG2 cell relative to the control; whereas, histone deacetylase 4, 7 (HDAC4, HDAC7), NUCB1, and TNNC1 were downregulated (Fig. 2). The data supported a strong consistency between the qPCR result and proteomic data.

Functional categorization of Luks-PV-regulated proteins

In order to identify the possible functions of these DEPs, thus we conducted the GO analysis to generate classification clusters. The results indicated that these proteins were mostly related to metabolisms and immune responses. As revealed in Fig. 3, the 'binding' (79 upregulated, 41 downregulated) and 'catalytic activity' (34 upregulated, 15 downregulated) were regarded as the most significant GO categories. Furthermore, the potential targets of LukS-PV were notably associated with transporter activity, signal transducer activity, molecular function regulator, structural molecule activity, and molecular transducer activity, whether the upregulated or downregulated DEPs. Additionally, several downregulated DEPs were found to only have electron carrier activity (1), protein tag (1), or nucleic acid binding transcription factor activity (1), while antioxidant activity (2) or transcription factor activity protein binding (2) was only possessed by several upregulated DEPs. In general, signal transduction and metabolic pathways related to LukS-PV may play important roles in favoring malignant phenotype reversion of HepG2 cells.

Fig. 3

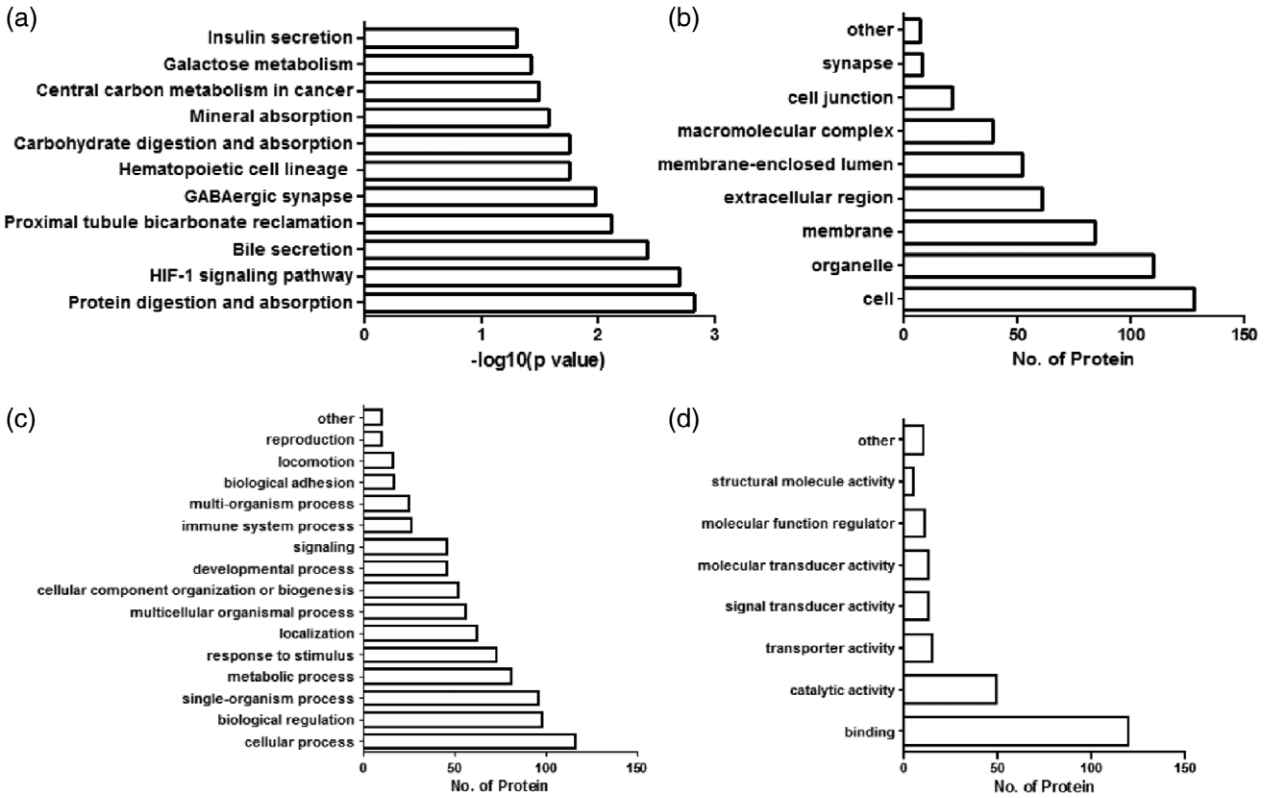

KEGG pathway and GO enrichment analysisof DEPs in HepG2 cells. (a) KEGG pathway; (b) cellular component; (c) biological process; (d) molecular functions. DEPs, differentially expressed proteins, KEGG, Kyoto Encyclopedia of Genes and Genomes.

Fig. 4

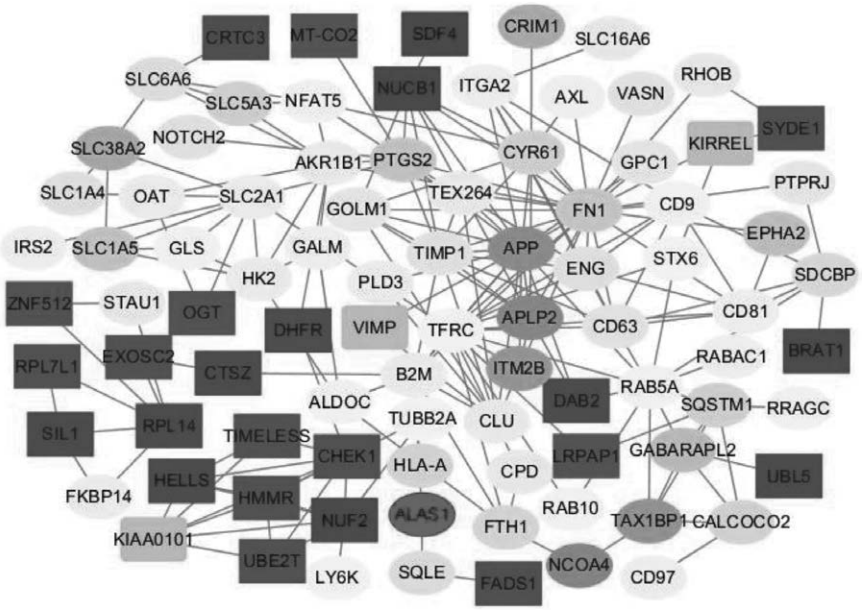

The protein–protein interactome networks. Blue rectangle nodes represent downregulated proteins. Red circular nodes stand for the upregulated proteins. The deeper the color, the obvious the fold change. The lines represent the regulation of relationship between two nodes.

Fig. 5

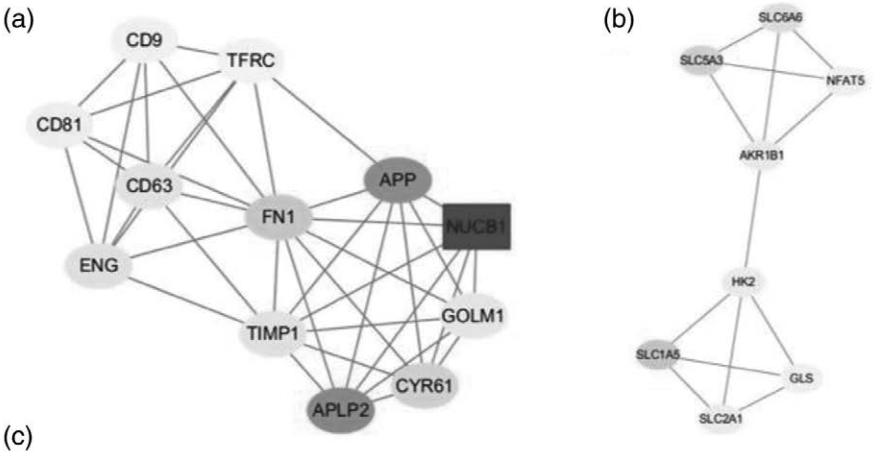

(c)

	KEGG pathway	Genes	P-Value
Module 1	Hematopoietic cell lineage	CD9, TFRC	6.50E-02
	HIF-1 signaling pathway	TIMP1, TFRC	8.00E-02
Module 2	Central carbon metabolism in cancer	GLS, HK2, SLC1A5, SLC2A1	2.90E-06
	Galactose metabolism	AKR1B1, HK2	1.80E-02
	Fructose and mannose metabolism	AKR1B1, HK2	1.80E-02
	HIF-1 signaling pathway	HK2, SLC1A1	5.70E-02

Top two modules from the PPI interaction networks. (a) Module 1; (b) module 2; (c) KEGG pathway analysis of proteins in modules 1 and 2. PPI, protein–protein interactome, KEGG, Kyoto Encyclopedia of Genes and Genomes.

Predicting protein–protein interactome networks and module analysis

Finally, protein–protein interaction networks were constructed using the online software STRING in combination with Cytoscape. The networks indicated a distinct set of interactions (Fig. 4). The top 10 proteins ranked by the MCC method were identified by CytoHubba plugin, including FN1, APP, TIMP1, NUCB1, GOLM1, APLP2, CYR61, CD63, ENG, and CD9, with most of them being upregulated, except for NUCB1. Additionally, modules of proteins in PPI networks were identified by the MCODE plugin in Cytoscape, following which, the top two notable modules were chosen for bioinformatics analysis. Functional enrichment analysis indicated that the module proteins were enriched in central carbon metabolism in cancer, galactose metabolism, and fructose and mannose metabolism (Fig. 5).

Discussion

In this study, we first demonstrated that LukS-PV could not only induce the apoptosis but also inhibit the proliferation, invasion, and metastasis in HCC cell line HepG2 cells. Our findings primarily revealed previously unrecognized effect of LukS-PV, and provided a potential agent for treating human HCC. We then analyzed the proteomes of the control and LukS-PV-treated HepG2 cells using LC-MS/MS. A total of 134 DEPs, including 88 upregulated and 46 downregulated were identified to be differentially expressed. The sensitivity of the DEP is evaluated based on the fold changes of protein as LukS-PV varies the effect on different proteins. Among the top 10 upregulated and 10 downregulated DEPs, we confirmed several protein level changes previously identified in human HCC, including PCLAF [13], NUF2 [14], and TAX1BP1 [15]. In particular, we identified novel candidate proteins such as ALAS1, NCOA4, ITM2B, SLC38A2, NUCB1, APLP2, APP, CRIM1, SDF4, TMEM59, TPBG, BRAT1, UBL5, SIL1, and three different histone H1 variants (H1F0, HIST1H1B, and HIST1H1D), with no relevant research reports, or of unknown function in HCC. Thus, it will be exciting to explore how gains or losses of their expression impact HCC progression.

Many studies have indicated that HCC is a metabolic disease. Our study from GO analysis and KEGG analysis found that central carbon metabolism in cancer was one of

the mostly affected pathways in KEGG analysis. Alterations in cancer central carbon metabolism including aerobic glycolysis, elevated glutaminolysis, dysregulated tricarboxylic acid cycle and pentose phosphate pathway, and facilitate cancer development by maintaining viability and building new biomass. Accumulating evidence suggests that a variety of oncogenes or tumor suppressors contribute to orchestrate the tightly controlled regulation of cancer metabolic adaptations, broadening the biological mechanisms of cancer metabolic reprogramming. Glutaminase (GLS), which converts glutamine to glutamate, plays a key role in cancer cell metabolism, growth, and proliferation. Yu *et al.* [16] found that high expression of GLS1 in HCC correlated with survival time of HCC patients. We found that GLS1 was upregulated in the response to LukS-PV treatment. Besides metabolism, these DEPs also participated in immunoregulation activities including biological regulation, response to stimulus, signaling, immune system process, and biological adhesion. These immune regulatory pathways were widely researched and demonstrated to be associated with HCC. Therefore, it is reasonable to propose that the aberrantly expressed proteins adjusted the progression of HCC, through affecting their correlated metabolic or immunological proteins.

This study also attempts to determine the downstream effector proteins that may interact with LukS-PV by PPI network. We predicted the top 10 most likely proteins, that is, proteins FN1, APP, TIMP1, NUCB1, GOLM1, APLP2, CYR61, CD63, ENG, and CD9. Among which, significant correlations of CYR61 [17], TIMP-1 [18], FN1 [19], ENG [8,20], and GOLM1 [21] with HCC were previously demonstrated through lipid metabolism, transportation, metastasis, proliferation, and angiogenesis, etc. Furthermore, proteins HK2, GLS, NFAT5, SLC1A5, SLC2A1, SLC5A3, and SLC6A6 were predicted to be associated specifically with AKR1B1. Further pathway analysis indicated that the protein was mostly related to galactose metabolism, and fructose and mannose metabolism. It has been reported that AKR1B1 overexpression in some types of HCCs might play a crucial role in the development of HCC [10,22]. However, another study indicated that AKR1B1 gene was significantly hypermethylated and downregulated in the HCC tumors compared with the nontumor liver tissues [11]. We found that AKR1B1 was elevated 1.698-fold in HepG2 cells after LukS-PV treatment. We presumed that protein AKR1B1 regulates the expression of certain proteins such as nuclear thyroid hormone receptor [22], and eventually affect the procedures of metabolism process to control the tumorigenesis.

Although no obvious correlation was found between LukS-PV treatment and HIF-1 signaling pathway, they appear to be related. For example, it was reported that activation expression of HIF-1 alpha retards tumor growth of renal cell carcinoma [23], implying that LukS-PV may play a tumor-suppressing role in the development and progress of HCC. However, paradoxically enough, previous studies indicated the oncogenic effects of HIF-1 signaling [24,25]. We hypothesized that the dual effects of HIF-1 signaling would allow optimal response to hypoxia by different types of cells. In short, therapeutic approaches to targeting of the HIF-1 signaling will need to take account of the particular setting.

NUCB1, also known as Calnuc, is a noteworthy protein. It is a multifunctional protein widely expressed in tissues and cells. In the Golgi, NUCB1 plays an important role in modulating Ca2+ homeostasis and is a negative regulator of the unfolded protein response through inhibition of site-1 protease-mediated cleavage of ATF6 [26]. Overexpression of NUCB1 might be associated with the activation or proliferation of the tumor cells. For example, Wang *et al.* [27] has demonstrated that in 50 gastric adenocarcinomas with lymph node metastasis, 56% of cases showed a positive reaction to Calnuc, which was much higher compared with that in 50 gastric adenocarcinomas without lymph node metastasis (10%). Another study indicates that aberrant Calnuc expression might contribute to the malignant transformation of colon cancer [28]. In the present study, we found that NUCB1 showed significantly lower expression HepG2 cells under LukS-PV treatment. It is speculated that LukS-PV might exert blocking and inhibiting HCCs effect through downregulating NUCB1 expression. However, no study has investigated the possible relationship of NUCB1 to HCC currently. For a better understanding of the correlation, more extensive study is needed.

In conclusion, we ascertained preliminarily that LukS-PV exerts antitumor effect in HCC hepatocarcinoma cells and identified a panel of dysregulated proteins for the HepG2 cell subjected to Luks-PV. Through data mining using GO analysis, which systematically presented the molecular functions and signaling pathways associated with the control of HCC. Further research is required to focus on the clinical application of these proteins and pathways for diagnosing, treating, and monitoring the prognosis of HCC.

Acknowledgements

This study was supported by 'the Fundamental Research Funds for the Central Universities' (WK9110000007). The funder played no role in the study design, data collection and analysis, decision to publish, or preparation of the manuscript.

All procedures performed in studies involving human participants were in accordance with the ethical standards of the institutional and/or national research committee and with the 1964 Helsinki declaration and its later amendments or comparable ethical standards.

Informed consent was obtained from all individual participants included in the study.

Conflicts of interest

There are no conflicts of interest.

References

1 Chen C, Lou T. Hypoxia inducible factors in hepatocellular carcinoma. *Oncotarget* 2017; **8**:46691–46703.
2 Attwa MH, El-Etreby SA. Guide for diagnosis and treatment of hepatocellular carcinoma. *World J Hepatol* 2015; **7**:1632–1651.
3 Sun XX, Zhang SS, Dai CY, Peng J, Pan Q, Xu LF, Ma XL. Luks-PV-regulated microrna-125a-3p promotes THP-1 macrophages differentiation and apoptosis by down-regulating NF1 and bcl-2. *Cell Physiol Biochem* 2017; **44**:1093–1105.
4 Zhang P, Yu WW, Peng J, Xu LF, Zhao CC, Chang WJ, Ma XL. Luks-PV induces apoptosis in acute myeloid leukemia cells mediated by C5A receptor. *Cancer Med* 2019; **8**:2474–2483.
5 Dai C, Zhang C, Sun X, Pan Q, Peng J, Shen J, Ma X. Luks-PV induces differentiation by activating the ERK signaling pathway and c-JUN/c-FOS in human acute myeloid leukemia cells. *Int J Biochem Cell Biol* 2016; **76**:107–114.
6 Hu WH, Hu Z, Shen X, Dong LY, Zhou WZ, Yu XX. C5A receptor enhances hepatocellular carcinoma cell invasiveness via activating ERK1/2-mediated epithelial-mesenchymal transition. *Exp Mol Pathol* 2016; **100**:101–108.
7 Wei X, Nie S, Liu H, Sun J, Liu J, Li J, *et al*. Angiopoietin-like protein 2 facilitates non-small cell lung cancer progression by promoting the polarization of M2 tumor-associated macrophages. *Am J Cancer Res* 2017; **7**:2220–2233.
8 Ho JW, Poon RT, Sun CK, Xue WC, Fan ST. Clinicopathological and prognostic implications of endoglin (CD105) expression in hepatocellular carcinoma and its adjacent non-tumorous liver. *World J Gastroenterol* 2005; **11**:176–181.
9 Wiśniewski JR, Zougman A, Nagaraj N, Mann M. Universal sample preparation method for proteome analysis. *Nat Methods* 2009; **6**:359–362.
10 Albrethsen J, Miller LM, Novikoff PM, Angeletti RH. Gel-based proteomics of liver cancer progression in rat. *Biochim Biophys Acta* 2011; **1814**:1367–1376.
11 Yamada N, Yasui K, Dohi O, Gen Y, Tomie A, Kitaichi T, *et al*. Genome-wide DNA methylation analysis in hepatocellular carcinoma. *Oncol Rep* 2016; **35**:2228–2236.
12 Karaosmanoğlu O, Banerjee S, Sivas H. Identification of biomarkers associated with partial epithelial to mesenchymal transition in the secretome of slug over-expressing hepatocellular carcinoma cells. *Cell Oncol (Dordr)* 2018; **41**:439–453.
13 Gai X, Tu K, Li C, Lu Z, Roberts LR, Zheng X. Histone acetyltransferase PCAF accelerates apoptosis by repressing a GLI1/BCL2/BAX axis in hepatocellular carcinoma. *Cell Death Dis* 2015; **6**:e1712.
14 Liu Q, Dai SJ, Li H, Dong L, Peng YP. Silencing of NUF2 inhibits tumor growth and induces apoptosis in human hepatocellular carcinomas. *Asian Pac J Cancer Prev* 2014; **15**:8623–8629.
15 Nguyen H, Sankaran S, Dandekar S. Hepatitis C virus core protein induces expression of genes regulating immune evasion and anti-apoptosis in hepatocytes. *Virology* 2006; **354**:58–68.
16 Yu D, Shi X, Meng G, Chen J, Yan C, Jiang Y, *et al*. Kidney-type glutaminase (GLS1) is a biomarker for pathologic diagnosis and prognosis of hepatocellular carcinoma. *Oncotarget* 2015; **6**:7619–7631.
17 Chen CC, Kim KH, Lau LF. The matricellular protein CCN1 suppresses hepatocarcinogenesis by inhibiting compensatory proliferation. *Oncogene* 2016; **35**:1314–1323.
18 Sung MT, Hsu HT, Lee CC, Lee HC, Kuo YJ, Hua K, *et al*. Krüppel-like factor 4 modulates the migration and invasion of hepatoma cells by suppressing TIMP-1 and TIMP-2. *Oncol Rep* 2015; **34**:439–446.
19 Schmitmeier S, Markland FS, Schönthal AH, Chen TC. Potent mimicry of fibronectin-induced intracellular signaling in glioma cells by the homodimeric snake venom disintegrin contortrostatin. *Neurosurgery* 2005; **57**:141–53; discussion 141.
20 Kasprzak A, Adamek A. Role of endoglin (CD105) in the progression of hepatocellular carcinoma and anti-angiogenic therapy. *Int J Mol Sci* 2018; **19**: E3887.
21 Zhang S, Ge W, Zou G, Yu L, Zhu Y, Li Q, *et al*. Mir-382 targets GOLM1 to inhibit metastasis of hepatocellular carcinoma and its down-regulation predicts a poor survival. *Am J Cancer Res* 2018; **8**:120–131.
22 Liao CS, Tai PJ, Huang YH, Chen RN, Wu SM, Kuo LW, *et al*. Regulation of AKR1B1 by thyroid hormone and its receptors. *Mol Cell Endocrinol* 2009; **307**:109–117.
23 Raval RR, Lau KW, Tran MG, Sowter HM, Mandriota SJ, Li JL, *et al*. Contravsting properties of hypoxia-inducible factor 1 (HIF-1) and HIF-2 in von hippel-lindau-associated renal cell carcinoma. *Mol Cell Biol* 2005; **25**:5675–5686.
24 Acker T, Diez-Juan A, Aragones J, Tjwa M, Brusselmans K, Moons L, *et al*. Genetic evidence for a tumor suppressor role of HIF-2alpha. *Cancer Cell* 2005; **8**:131–141.
25 Kung AL, Wang S, Klco JM, Kaelin WG, Livingston DM. Suppression of tumor growth through disruption of hypoxia-inducible transcription. *Nat Med* 2000; **6**:1335–1340.
26 Tsukumo Y, Tomida A, Kitahara O, Nakamura Y, Asada S, Mori K, *et al*. Nucleobindin1 controls the unfolded protein response by inhibiting ATF6 activation. *J Biol Chem* 2007; **282**:29264–29272.
27 Wang SN, Miyauchi M, Koshikawa N, Maruyama K, Kubota T, Miura K, *et al*. Antigen expression associated with lymph node metastasis in gastric adenocarcinomas. *Pathol Int* 1994; **44**:844–849.
28 Chen Y, Lin P, Qiu S, Peng XX, Looi K, Farquhar MG, Zhang JY. Autoantibodies to ca2+ binding protein calnuc is a potential marker in colon cancer detection. *Int J Oncol* 2007; **30**:1137–1144.